The chromatic eye: a new reduced-eye model of ocular chromatic aberration in humans

Larry N. Thibos, Ming Ye, Xiaoxiao Zhang, and Arthur Bradley

New measurements of the chromatic difference of focus of the human eye were obtained with a two-color, vernier-alignment technique. The results were used to redefine the variation of refractive index of the reduced eye over the visible spectrum. The reduced eye was further modified by changing the refracting surface to an aspherical shape to reduce the amount of spherical aberration. The resulting chromatic-eye model provides an improved account of both the longitudinal and transverse forms of ocular chromatic aberration.

Key words: Chromatic aberration, visual optics, schematic eye.

Introduction

The optical apparatus of the eye represents a low-pass spatial filter at the front end of the visual system, which is a potential limiting factor for any visual task. In the well-focused eye, chromatic aberration and diffraction are thought to be two of the major optical factors that limit visual performance.[1-3] Recent evidence indicates that ocular chromatic aberration can significantly reduce image contrast which results in loss of contrast sensitivity and visual acuity, and may also inject large artifacts into the retinal image of colored visual targets.[4,5] Such problems can be greatly exaggerated by the misalignment of achromatizing lenses[6] or other optical apparatus, such as clinical Maxwellian-view systems.[7] Any visually coupled device that shifts the eye's achromatic axis away from the fovea will expose central vision to transverse chromatic aberration, which is typically absent or very small (<1 arcmin) in normal eyes.[8,9] To help gauge the potential magnitude and significance of these optical effects for visual performance, it is important to have available an accurate, mathematically tractable model of ocular chromatic aberration of the human eye.

Since the time of Helmholtz the eye's variation of focal power with wavelength[10-12] has been modeled by a reduced schematic eye[13] that consists of a volume of water encased within a single, spherical refracting surface. The chromatic aberration of the reduced eye is attributed solely to the variation of the refractive index of water with wavelength. By including a pupil in the model the reduced eye also accounts for two forms of transverse aberration: chromatic difference of magnification[14] and chromatic difference of position.[9] Calculation of the optical image quality is particularly easy with such a simple physical model, especially if the model's spherical aberration is ignored. Such calculations have been used to predict the effects of ocular chromatic aberration on several aspects of visual performance.[3,15,16]

Although the reduced eye accounts well for the major features of ocular chromatic aberration in human eyes, there are at least three ways in which the model might be improved. First, published measurements of the magnitude of chromatic aberration have consistently shown that the model does not fit the data well for short wavelengths of light.[9-12] Second, the traditional model has a large amount of spherical aberration, which causes a nonlinear relationship between transverse chromatic aberration and pupil location that is not always evident in the data.[9] Third, the underlying data that support the model might be improved. The psychophysical method of best focus that is traditionally used to measure chromatic aberration may not be as reliable as Ivanoff's two-color vernier method[17] for several reasons[18]: (1) Because it is a hyperacuity task, vernier alignment has inherently less measurement error than that typically obtained with other visual tasks. (2) Vernier acuity is less dependent on changes in wavelength than is the method of best focus. (3) The task of adjusting a point source to be maximally distinct is more vulnerable to criterion differences

The authors are with the Department of Visual Sciences, School of Optometry, Indiana University, Bloomington, Indiana 47405.

Received 24 June 1991.
0003-6935/92/193594-07$05.00/0.

across subjects than is a vernier task. (4) The best focus method is subject to contamination by optical aberrations other than defocus that affect the distinctness of the image. This latter problem is exacerbated by the requirement for a large pupil to minimize the depth of focus.

The present study is an attempt to improve the accuracy and reliability of the reduced-eye model by refining the specification of how the refractive index of the model's optical medium varies with wavelength. Our plan was to measure experimentally the chromatic variation of refractive error in human eyes by the two-color vernier method and from these data infer the necessary variation of refractive index for the model. In addition we sought to reduce the model's spherical aberration by giving the refracting surface an aspherical shape. The motivation for this change was to put the model in closer agreement with previous experimental data and, at the same time, justify the useful simplification of ignoring the spherical aberration when calculating optical image quality.

Methods

The principle of the two-color vernier method[9,17] for measuring focusing errors of the eye is illustrated in Fig. 1. A subject viewed a vertically oriented, vernier target in which the upper bar was fixed in space and illuminated with the light of a reference wavelength of 555 nm. The lower bar of the target could be displaced horizontally and was illuminated with a variable wavelength source. The vernier targets were produced by backilluminating diffusing glass with white light. Movable rectangular apertures formed the bars of the target, and each aperture carried an interference filter. Because of the eye's differential sensitivity across the visible spectrum, target luminance varied with test wavelength over a range of 61 cd/m^2 (middle wavelengths) to 1 cd/m^2 (short or long test wavelengths). To compensate, a neutral density filter was included in the reference aperture so that the luminance of the two bars in the target would always match. Twelve test wavelengths were nominally spaced at 25-nm intervals over the visible spectrum (400–700 nm), thus covering the range of importance over which relative human spectral sensitivity V_λ varies from $<1\%$ to 100%.

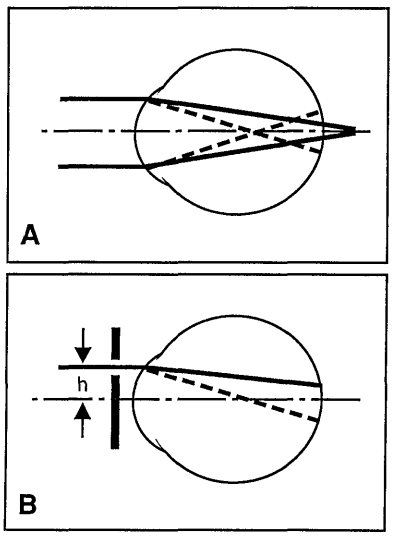

Fig. 1. Principle of the two-color vernier method for measuring ocular chromatic aberration. A, ocular media have greater refractive indices for short wavelengths (dashed rays) than for long (solid rays), which results in a chromatic difference of focus. B, by isolating marginal rays with a pinhole aperture, a focusing difference becomes a difference in image location that can be measured with a vernier target. The amount of vernier misalignment is proportional to displacement h of the pinhole from the visual axis and to the chromatic difference in the refractive error of the eye.

Eight subjects (ranging in age from 30 to 42 yr) were tested by using either the right or left eye. Refractive errors (0–5-D myopia) were left uncorrected, pupils were dilated, and accommodation was relaxed (0.5% cyclopentalate hydrochloride). The viewing distance was 2 m, and each bar of the vernier target subtended 3.5 × 58.5 arc min. The subject viewed the target through a pinhole aperture that was attached to a micrometer, which allowed precise positioning by the experimenter. The pinhole diameter was 0.7 mm, and measurement accuracy for vernier offset was 5 arc sec. The subject's task was to align the two-color vernier target by misaligning physically the lower bar in compensation for the chromatic difference in the image position illustrated in Fig. 1B. In the context of the reduced-eye model the amount of defocus of the eye for the given test wavelength is given by the rate of change of the vernier offset with pinhole displacement.[9,17] Previous experiments have confirmed[8,9] that this rate of change is constant within the paraxial region (±1.5-mm pinhole displacement).

To place the pinhole in the paraxial region it was first necessary to locate the foveal achromatic axis, which is defined as the axis for which there is zero transverse chromatic aberration for foveal viewing.[12] One point on this reference axis is the fixation point, and a second was found empirically by first positioning the pinhole horizontally so that a vertical, red-blue vernier target appears aligned when physically aligned. This procedure was then repeated for vertical movement of the pinhole, and a horizontal vernier target and the final location thus established the achromatic condition that defines the axis. Next, the pinhole was placed at each of three paraxial locations relative to the reference axis for the experiment: on axis, 1.5 mm nasal, and 1.5 mm temporal. At each location a minimum of five settings of the vernier target were recorded for each test wavelength. The complete experiment was repeated for 12 test wavelengths for each of eight subjects.

A second series of experiments was conducted on five of the same subjects to explore a wider range of pinhole locations. In this series the two wavelengths used in the vernier target were fixed at 433 and 622 nm.

Modeling

For Emsley's[13] reduced eye the relationship between the axial refractive error ΔR_x and the refractive index of the medium $n(\lambda)$ for a given test wavelength λ is given by[3]

$$\Delta R_x = \frac{n_{\text{ref}} - n(\lambda)}{r \cdot n_{\text{D}}}, \tag{1}$$

where n_{ref} is the index at the experimental reference wavelength (555 nm), $n_{\text{D}} = 1.333$ is the index at the model's emmetropic wavelength (589 nm is the sodium D line), and r is the radius of curvature (5.55 mm) of the refracting surface. Le Grand[19] suggests the use of Cornu's hyperbolic formula for the refractive index of water:

$$n(\lambda) = a + b/(\lambda - c), \tag{2}$$

where λ is in micrometers and the other parameters are $a = 1.31848$, $b = 0.006662$, and $c = 0.1292$. Since ΔR_x is a linear function of $n(\lambda)$, it follows that the variation of absolute refractive error with wavelength will also be a hyperbolic function of the form

$$R_x = p - q/(\lambda - c). \tag{3}$$

By refining the reduced-eye model our initial goal was to determine the three parameters of the refractive-index function $n(\lambda)$ by a least-squares fitting procedure while leaving all other aspects of the model unchanged. Then, once the optical medium was defined in this way, we exchanged the spherical refracting surface for one of elliptical shape but with the same axial radius of curvature r as the traditional spherical model (see Appendix A). With this design both models have the same axial optical power, and thus the above equations apply equally well to each.

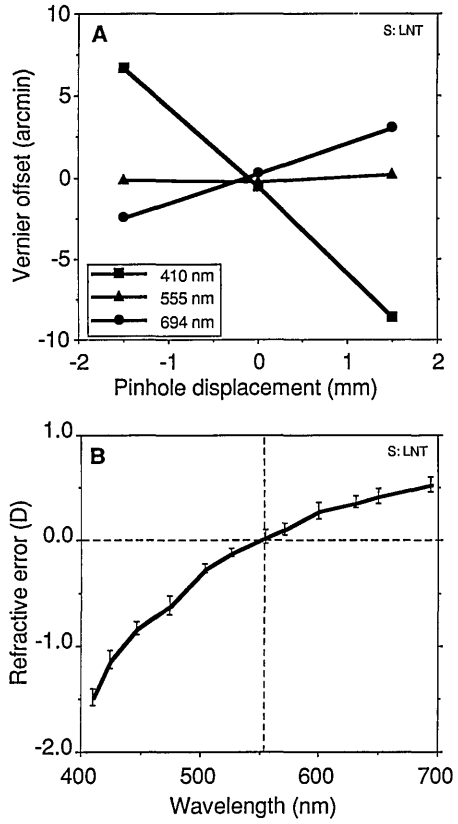

Fig. 2. Typical experimental results for one of eight subjects. A, mean ($n = 5$) results for the two-color vernier task are shown for three of 12 wavelengths tested. Standard errors of the means are less than the symbol radius. The slope of each line is a measure of the chromatic refractive error for the given wavelength relative to 555 nm. Pinhole displacement is from the empirically determined foveal achromatic axis. B, variation of the refractive error with the wavelength. Error bars show ±2 standard errors of dioptric value estimates that are obtained by linear regression of the individual data lines in the format shown in A.

Results

The basic experiment was to measure how the vernier offset varies with pinhole displacement for the two-color vernier alignment task. This experiment was conducted for 12 test wavelengths and for eight subjects. Results were consistent across subjects, and typical data are shown in Fig. 2A for three test wavelengths that represent the middle and two ends of the visible spectrum. As expected from previous experiments of this kind,[9] the variability of the vernier settings was extremely low. The standard deviation of repeated settings was in the 15–30-arc sec range for all subjects. The slope of each line, obtained by linear regression, was interpreted as the magnitude of refractive error for the given wavelength and was expressed in dioptric terms by converting the experimental units of arc min/mm to rad/m. Figure 2B summarizes how the refractive error varies with wavelength for this subject. The reliability of the estimated refractive errors was very high as may be judged from the small error bars, which represent ±2 standard errors of the estimated (regression) slope. For the data of subject LNT, which are shown in Fig. 2B, the maximum standard error of the refractive error was 4.6 arc sec/mm = 0.02 D, and the range of errors for all eight subjects was 0.01–0.06 D.

Little intersubject variability was found as may be seen from the pooled results for all subjects in Fig. 3. The differences between subjects were of the same order as the variability of data for individual subjects (maximum standard error of the mean < 0.04 D), and therefore the data were averaged across subjects for further analysis. Interpolation of the mean results indicated that the difference in refractive error between 555 nm (the experimental reference wavelength) and 589 nm (the emmetropic wavelength of the water eye) was 0.21 D. Therefore, we subtracted 0.21 from all the mean data and interpreted the result as the absolute refractive error of the model eye, as shown by solid circles in Fig. 4. Next, mean refractive errors were converted to refractive-index values for the optical medium of the model eye by application of Eq. (1), and these results are shown by the solid squares of Fig. 4. The latter were then fit with a hyperbolic curve of the form given by Eq. (2), and the resulting regression coefficients were $a = 1.320535$

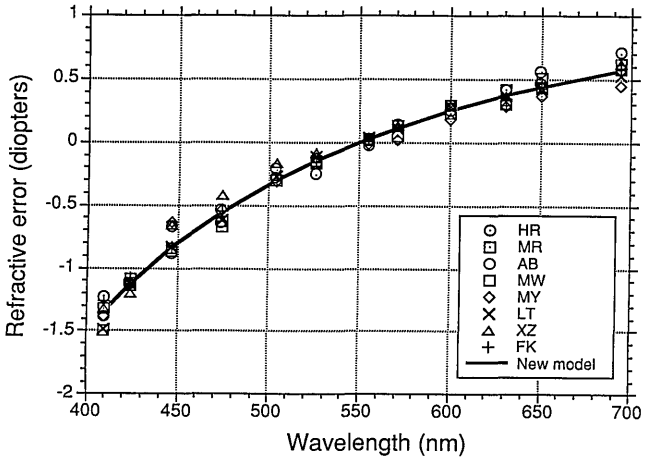

Fig. 3. Ocular chromatic aberration for eight subjects. The symbols show the mean refractive errors that are relative to 555 nm. The curve is a least-squares fit of a hyperbolic curve that describes the chromatic-eye model [see Eq. (3)].

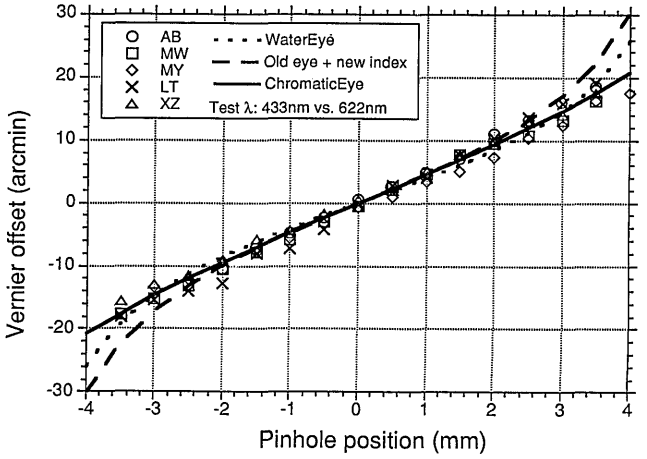

Fig. 5. Induced transverse chromatic aberration at fixed wavelengths (433, 622 nm) for five subjects. Results are compared with predictions from three versions of the reduced-eye model.

(standard error = 0.000921), $b = 0.004685$ (standard error = 0.000546), $c = 0.214102$ (standard error = 0.016202). From these results we calculate that the parameters of Eq. (3) for the absolute refractive error of the model have values of $p = 1.68524$, $q = 0.63346$, and $c = 0.21410$ when R_x is in diopters and λ is in micrometers.

To provide evidence that would further discriminate between the various models being considered, we explored the nonparaxial range of pinhole locations in a second series of experiments on five subjects for fixed vernier wavelengths. The results are shown in Fig. 5 along with the predictions for the original Emsley reduced eye, the Emsley eye filled with the newly defined optical medium, and our proposed new model that has the new medium plus an aspherical

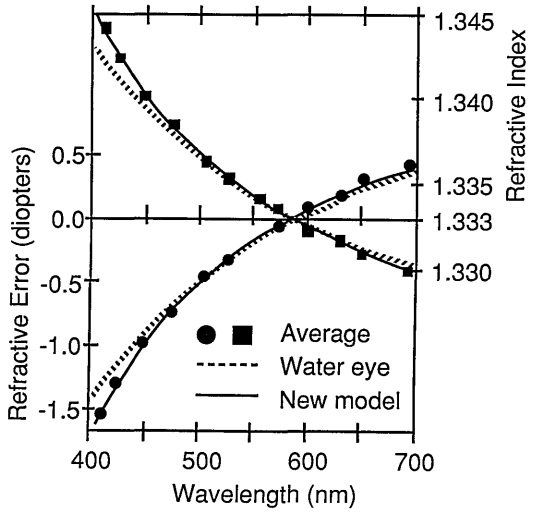

Fig. 4. Comparison of mean results with two models: Emsley's water eye (dotted curve) and the same model filled with a different refracting medium (solid curve). Symbols show the mean refractive error (●) and the calculated refractive index (■) based on the data of Fig. 3 for eight subjects. Standard errors are less than the symbol radius.

refracting surface. Although there is little to distinguish these models in the paraxial region, for large pinhole displacements the new model is a better predictor of the data.

Discussion

The results of these experiments provide a reliable new assessment of the variation of refractive error of the human eye across the visible spectrum. The data are accurately described by a reduced-eye optical model that has a refractive index that changes more rapidly with the wavelength than occurs for water. The comparisons drawn in Fig. 4 clearly show the improvements that are gained in describing chromatic errors of focus, especially at the shorter wavelengths, simply by changing the ocular medium while leaving all other aspects of the model unchanged.

A retrospective comparison of the predictions of the new model with previously published data[10–12,20–28] is provided in Fig. 6. To enable the comparison all the data were put on a common basis by referencing the error to a common wavelength (589 nm). When compared in this way there is remarkably little difference between the results. Of the 12 previous studies, only Ivanoff used the two-color vernier technique. Present results confirm and extend his observation that data obtained by the vernier technique and the method of best focus are in good agreement despite the potential problems that are identified in the Introduction.

Although predictions of the eye's chromatic difference in refractive error are improved by changing the refractive medium in Emsley's reduced-eye model, the predictions of induced transverse chromatic aberration are worse. The relatively poor performance that is evident in Fig. 5 for the revised model is due to the large amount of spherical aberration that is present. To improve the prediction of the transverse form of chromatic aberration, we modified the reduced eye further by making the refracting interface a surface of revolution of an ellipse (i.e., a prolate

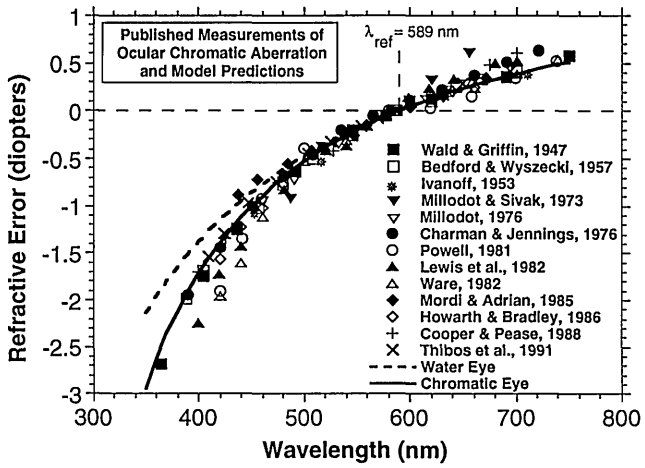

Fig. 6. Comparison of published measurements of ocular chromatic aberration with the traditional water-eye model and with the new chromatic-eye model. Published results were put on a common basis by translating data points vertically until the refractive error was zero at the reference wavelength (589 nm).

spheroid). As described in Appendix A, such a model has zero spherical aberration for distant objects at the emmetropic wavelength (589 nm) and has only minor amounts at other wavelengths. Consequently the transverse chromatic aberration that is induced by a displaced pinhole is a nearly linear function in the nonparaxial as well as the paraxial region and thus matches the data more closely. Since we chose an elliptical surface with the same vertex curvature as in Emsley's model, the change in surface shape will not disturb the excellent fit of the model to the axial refractive error data in Figs. 4 and 6.

Changing to an aspherical refracting surface for the reduced eye creates an optical axis of symmetry that is absent from earlier models. The traditional model has a spherical surface and no pupil and thus has no inherent axis of symmetry.[13] To account for transverse chromatic aberration, Thibos[29] introduced a pupil into the model thus creating a reference axis that is defined by the center of the pupil and the center of curvature of the refracting surface (the nodal point). This reference axis was subsequently termed the achromatic axis of the eye since it locates that unique point of the retinal image that is subject to zero transverse chromatic aberration.[9] The achromatic axis is defined in the same way for the new aspherical model, but in addition the foci of the ellipse define an optical axis that contains the model's single nodal point but that does not necessarily contain either the center of the pupil or the fovea. However, given the close fit of the model to the data that are obtained with central vision (Fig. 5), it is reasonable to place the fovea of the model eye on the new optical axis as shown in Fig. 8, in which case the optical axis coincides with the visual axis.[9] If this convention is adopted, the proposed new model may aid in the modeling of foveal transverse chromatic aberration caused by pupil decentration.[8,9,30,31] A key parameter of this description will be the angle ψ between the visual axis and the achromatic axis.[9]

To distinguish it from the traditional water eye, we dubbed our new model the chromatic eye. In Fig. 7 a schematic diagram of the model is compared with Emsley's reduced eye. We anticipate that the chromatic-eye model will be useful for calculating polychromatic image quality since it represents an optical system that suffers only from the effects of (chromatic) defocus and diffraction by the pupil, at least within the paraxial region. Calculation of the optical transfer function by wave-optical methods is particularly easy for such a system.[32]

Appendix A

By Fermat's principle stigmatic imaging of a point source will occur when the optical path length is the same for all refracted rays. It follows that the reduced-eye model in Fig. 8 will have zero spherical aberration for the emmetropic wavelength when the refracting surface is defined by

$$x + n \cdot QF = n \cdot f', \tag{A1}$$

where n is the refractive index of the optical medium of the model, f' is the secondary focal length, and Q is an arbitrary point on the refracting surface. By applying the Pythagorean theorem, this equation

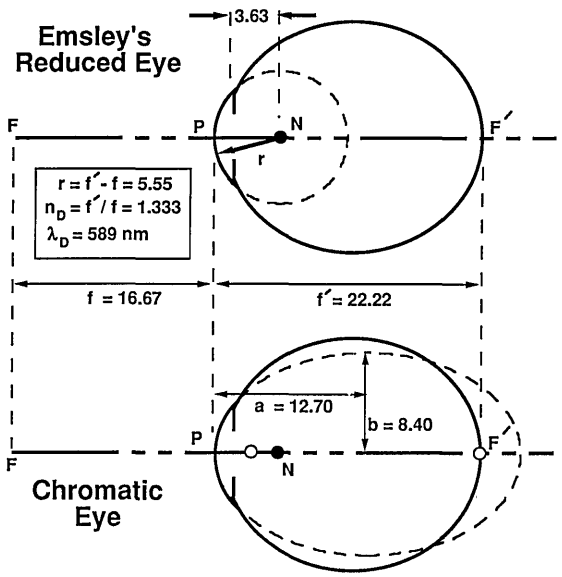

Fig. 7. Comparison of Emsley's reduced eye and the proposed chromatic eye. The refracting surface is a sphere for Emsley's model and a prolate spheroid for the chromatic eye, which corresponds, respectively, to a circle and an ellipse when viewed in cross section. Given f and f' from Gullstrand's schematic eye, Emsley's model is completely determined by the pair of equations shown. The surface of the new model is given by Eqs. (A2) and (A3). By using Eq. (2) for specifying the refractive index, the emmetropic wavelength is 589 nm for both models. Dashed lines indicate the continuation of the refracting surfaces. Solid circles show the nodal point, and dashed circles show the two foci of the ellipse. Both surfaces have a radius of curvature r at vertex point P. Distances shown are in millimeters.

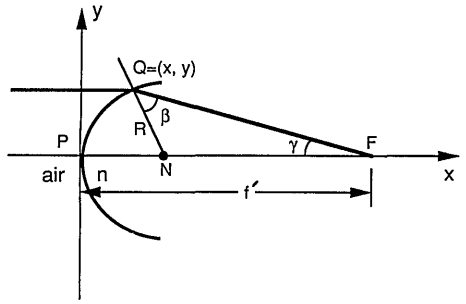

Fig. 8. Ray diagram for stigmatic imaging at F of a distant, axial point source. Q at (x, y) is an arbitrary point on the refracting surface; N is the nodal point. R is distance $\overline{QN}$; β and γ are included angles of triangle QNF.

may be placed in the following standard form:

$$\frac{(x-a)^2}{a^2}+\frac{y^2}{b^2}=1, \tag{A2}$$

where

$$a = nf'/(n+1),$$
$$b = f'[(n-1)/(n+1)]^{1/2}. \tag{A3}$$

Since a and b are both positive quantities, Eq. (A2) describes an ellipse with major and minor hemiaxes of length $a = 12.70$ mm and $b = 8.40$ mm, respectively, given $n = 1.333$ and $f' = 22.22$ mm. The ellipse is centered on the point $(a, 0)$, and the foci are at $[f'(n-1)/(n+1), 0]$ and $(f', 0)$.

The axial power of the elliptical refracting surface is determined by the radius of curvature ρ at the vertex point P. To show that both models in Fig. 7 have the same vertex radius of curvature (and thus the same nodal point), first we express the ellipse in parametric form:

$$x - a = a\cos(\theta),$$
$$y = b\sin(\theta), \tag{A4}$$

and then evaluate the usual formula[33] for ρ:

$$\rho = \frac{(\dot{x}^2+\dot{y}^2)^{3/2}}{\dot{x}\ddot{y}-\ddot{x}\dot{y}}, \tag{A5}$$

where the dotted variables indicate first and second derivatives with respect to θ. At the vertex $\theta = -\pi$, and thus Eq. (A5) simplifies to

$$\rho = f'(n-1)/n. \tag{A6}$$

The right-hand side of Eq. (A6) is recognized as an expression for the radius of curvature of the spherical refracting surface in Emsley's reduced eye. This follows from the fact that the optical power of a spherical refracting surface can be specified either as $(n-1)/r$ or as n/f'.

This research was supported by National Institutes of Health grant EY5109 to Larry N. Thibos and by U.S. Air Force Office of Scientific Research grant 870089 to the Indiana Institute for the Study of Human Capabilities. We thank Peter Howarth for motivating us to find a better optical model for chromatic aberration of the human eye.

References

1. A. van Meeteren, "Calculations on the optical modulation transfer function of the human eye for white light," Opt. Acta **21,** 395–412 (1974).
2. A. van Meeteren and C. J. W. Dunnewold, "Image quality of the human eye for eccentric entrance pupil," Vision Res. **23,** 573–579 (1983).
3. L. N. Thibos, A. Bradley, and X. Zhang, "The effect of ocular chromatic aberration on monocular visual performance," Optom. Vis. Sci. **68,** 599–607 (1991).
4. A. Bradley, X. Zhang, and L. N. Thibos, "Retinal image isoluminance is compromised by lateral and longitudinal chromatic aberration," in *OSA Annual Meeting* Vol. 11 of 1988 OSA Technical Digest Series (Optical Society of America, Washington, D.C., 1988), p. 47.
5. X. Zhang, A. Bradley, and L. N. Thibos, "Theoretical analysis of the effect of chromatic aberration on chromatic appearance of isoluminance color gratings," Optom. Vis. Sci. **66** (Suppl.), 220 (1989).
6. A. Bradley, X. Zhang, and L. N. Thibos, "Achromatizing the human eye," Optom. Vis. Sci. **68,** 608–616 (1991).
7. A. Bradley, L. N. Thibos, and D. L. Still, "Visual acuity measured with clinical Maxwellian-view systems: effects of beam entry location," Optom. Vis. Sci. **67,** 811–817 (1990).
8. P. Simonet and M. C. W. Campbell, "The optical transverse chromatic aberration on the fovea of the human eye," Vision Res. **30,** 187–206 (1990).
9. L. N. Thibos, A. Bradley, D. L. Still, X. Zhang, and P. A. Howarth, "Theory and measurement of ocular chromatic aberration," Vision Res. **30,** 33–49 (1990).
10. G. Wald and D. R. Griffin, "The change in refractive power of the human eye in dim and bright light," J. Opt. Soc. Am. **37,** 321–336 (1947).
11. R. E. Bedford and G. Wyszecki, "Axial chromatic aberration of the human eye," J. Opt. Soc. Am. **47,** 564–565 (1957).
12. A. Ivanoff, *Les Aberrations de l'Oeil* (Editions de la Revue d'Optique Theorique et Instrumentale, Paris, 1953).
13. H. H. Emsley, *Visual Optics* (Hatton, London, 1952).
14. X. Zhang, L. N. Thibos, and A. Bradley, "Relation between the chromatic difference of refraction and the chromatic difference of magnification for the reduced eye," Optom. Vis. Sci. **68,** 456–458 (1991).
15. L. N. Thibos, "Optical limitations of the Maxwellian-view interferometer," Appl. Opt. **29,** 1411–1419 (1990).
16. X. Zhang, A. Bradley, and L. Thibos, "Achromatizing the human eye: the problem of chromatic parallax," J. Opt. Soc. Am. A **8,** 686–691 (1991).
17. A. Ivanoff, "Sur une methode de mesure des aberrations chromatiques et spheriques de l'oeil en lumiere dirigee," C. R. Acad. Sci. **223,** 170–172 (1946).
18. P. Simonet and M. C. W. Campbell, "Accuracy and reliability of the chromatic parallax method for measuring the longitudinal chromatic aberration of the human eye," Optom. Vis. Sci. **67** (Suppl.), 55 (1990).
19. Y. Le Grand, *Form and Space Vision,* translated by G. G. Heath and M. Millodot (Indiana U. Press, Bloomington, Ind., 1967).
20. M. Millodot and J. G. Sivak, "Influence of accommodation on the chromatic aberration of the eye," Br. J. Physiol. Opt. **28,** 169–174 (1973).
21. M. Millodot, "The influence of age on the chromatic aberration

of the human eye," Graefe's Arch. Clin. Exp. Ophthalmol. **198,** 235–243 (1976).
22. W. N. Charman and J. A. M. Jennings, "Objective measurements of the longitudinal chromatic aberration the human eye," Vision Res. **16,** 99–1005 (1976).
23. I. Powell, "Lenses for correcting chromatic aberration of the eye," Appl. Opt. **20,** 4152–4155 (1981).
24. A. L. Lewis, M. Katz, and C. Oehrlein, "A modified achromatizing lens," Am. J. Optom. Physiol. Opt. **59,** 909–911 (1982).
25. C. Ware, "Human axial chromatic aberration found not to decline with age," Graefe's Arch. Clin. Exp. Ophthalmol. **218,** 39–41 (1982).
26. J. A. Mordi and W. K. Adrian, "Influence of age on the chromatic aberration of the human eye," Am. J. Optom. Physiol. Opt. **62,** 864–869 (1985).
27. P. A. Howarth and A. Bradley, "The longitudinal chromatic aberration of the human eye, and its correction," Vision Res. **26,** 361–366 (1986).
28. D. P. Cooper and P. L. Pease, "Longitudinal chromatic aberration of the human eye and wavelength in focus," Am. J. Optom. Physiol. Opt. **65,** 99–107 (1988).
29. L. N. Thibos, "Calculation of the influence of lateral chromatic aberration on image quality across the visual field," J. Opt. Soc. Am. A **4,** 1673–1680 (1987).
30. G. Walsh, "The effect of mydriasis on the pupillary centration of the human eye," Ophthal. Physiol. Opt. **8,** 178–182 (1988).
31. M. A. Wilson, M. C. W. Campbell, and P. Simonet, "Change of pupil centration with change of illumination and pupil size," Optom. Vis. Sci. **69,** 129–136 (1992).
32. H. H. Hopkins, "The frequency response of a defocused optical system," Proc. R. Soc. London Ser. A **231,** 91–103 (1955).
33. G. B. Thomas, *Calculus and Analytic Geometry* (Addison-Wesley, Reading, Mass., 1960).